COMITATO NAZIONALE PER L'ENERGIA NUCLEARE
Laboratori Nazionali di Frascati

LNF-68/22
9 Aprile 1968

G. Barbiellini, G. Capon, G. De Zorzi and G. P. Murtas : PROTON COMPTON EFFECT BY POLARIZED PHOTONS AT 90^{o} IN THE C. M. IN THE FIRST RESONANCE REGION. -

Servizio Documentazione
dei Laboratori Nazionali di Frascati del CNEN
Casella Postale 70 - Frascati (Roma)

Laboratori Nazionali di Frascati del CNEN
Servizio Documentazione

LNF-68/22

Nota interna: n. 396
9 Aprile 1968

G. Barbiellini, G. Capon, G. De Zorzi and G. P. Murtas: PROTON COMPTON EFFECT BY POLARIZED PHOTONS AT 90° IN THE C. M. IN THE FIRST RESONANCE REGION. -

(Submitted for publication to Physical Review)

ABSTRACT. -

For the reaction $\gamma + p \rightarrow \gamma' + p'$ (proton Compton effect) we have measured the ratio $d\sigma_{\parallel}/d\sigma_{\perp}$ between the cross sections for linearly polarized photons using the coherent bremsstrahlung beam of the Frascati electron synchrotron. At 90° in the C. M. and in the photon energy region $300 \leq K \leq 335$ MeV we find

$$d\sigma_{\parallel}/d\sigma_{\perp} = 2,1 \begin{matrix} +.5 \\ -.4 \end{matrix}$$

In absence of theoretical predictions in this energy region founded on the dispersive theory, this result is compared with the values obtained using an isobaric model, taking into account various possible intermediate states.

INTRODUCTION. -

A polarized γ ray beam[1] can provide further information on γ induced reactions. Such a beam is a facility of the Frascati 1 GeV electron synchrotron and a considerable amount of investigation on the pion photoproduction has already been carried out with it.

Experimental data on pion photoproduction cross sections are now relatively numerous and accurate, and information on production from polarized beams and on the polarization of the recoil nucleon is coming out. Moreover agreement between theory and experiment has been gradually improving in these last years as progress were made on both sides and nowadays there are many improvements on the original CGLN theory on photoproduction which are in satisfactory agreement with the most refined experimental data.

For Compton effect, instead, the experimental data, also because of experimental difficulties are less abundant and precise and are restricted only to the measurement of the cross sections; no experiments with polarized photons or on the recoil nucleon polarization having been done. The comparison between theory and experiment, which has been mainly made with dispersion theory technique and with the isobaric model, is not as satisfactory as in photoproduction.

It is then convenient to increase and improve the experimental data, in order to develop a more stringent comparison between theory and experiment for Compton effect. This can contribute to a better understanding of hadrons electromagnetic interactions.

Therefore we have measured the quantity $R\sigma = d\sigma_{\parallel}/d\sigma_{\perp}$ where $d\sigma_{\parallel}$ ($d\sigma_{\perp}$) are the cross sections for Compton scattering with the incoming photon polarized parallel (normal to the reaction plane).

Experiment is made at 90^{o} in C. M. and the R_{σ} value is given for the energy interval 300 - 335 MeV of the primary photon, where the beam polarization attains the maximum.

BEAM CHARACTERISTICS. -

The experiment has been performed using the polarized γ ray beam which is obtained using a diamond crystal as radiator. The properties of such a beam have been described in (1).

The crystal is oriented in such a way that the electron momentum $\vec{p}$, lies in the plane of the [110], [001] axes, at a small angle with respect to the [110] axis. Then the beam spectrum presents a peak of intensity, to which corresponds also the maximum polarization, at a photon energy dependent on the angle θ between $\vec{p}$

and the [110] axis.

The polarization is defined as:

$$P(K) = \frac{I_n(K) - I_p(K)}{I_n(K) + I_p(K)} \quad , \quad K: \text{photon energy}$$

I_n (I_p) being the intensity of photons with electric vector normal (parallel) to the [110] - [001] plane.

Data are collected using two diamonds: the plane [110] - [001] is vertical for the first one, horizontal for the second one.

In the first (second) case we have an excess of photons with polarization vector parallel: $\parallel$ (normal: $\perp$) to the reaction plane which is horizontal in our experiment.

Then if $C_{\parallel}$, $C_{\perp}$ are respectively the Compton counting rates for the two situations, one obtains the cross sections ratio via the formula:

$$\frac{d\sigma_{\parallel}}{d\sigma_{\perp}} = \frac{|P|\,(R_c + 1) + (R_c - 1)}{|P|\,(R_c + 1) - (R_c - 1)} \quad ; \quad R_c = \frac{C_{\parallel}}{C_{\perp}}$$

During the experiment the beam spectrum has been measured with a pair spectrometer of energy resolution $\Delta K/K = \pm 4\%$. The beam dose is measured with a Wilson quantameter.

In Fig. 1 are shown the spectra for the two diamonds as measured with the pair spectrometer.

Each one is the weighted mean of various measured spectra: the slight difference between them is due to the impossibility of reproducing exactly every time the position of the crystal.

In the following the counting rates are properly corrected for the small differences in the intensities.

For any orientation of the diamond it is possible to calculate theoretically the beam spectrum and polarization.

Fig. 2 shows the average spectrum, together with the theoretical spectrum which is in best agreement (this last one takes into account the experimental atomic form factor, Moliere multiple scattering in the diamond, electron beam proper divergence, collimation, energy resolution of the pair spectrometer). Besides is shown the theoretical polarization associated to this theoretical spectrum. This polarization is assumed to be the beam polarization.

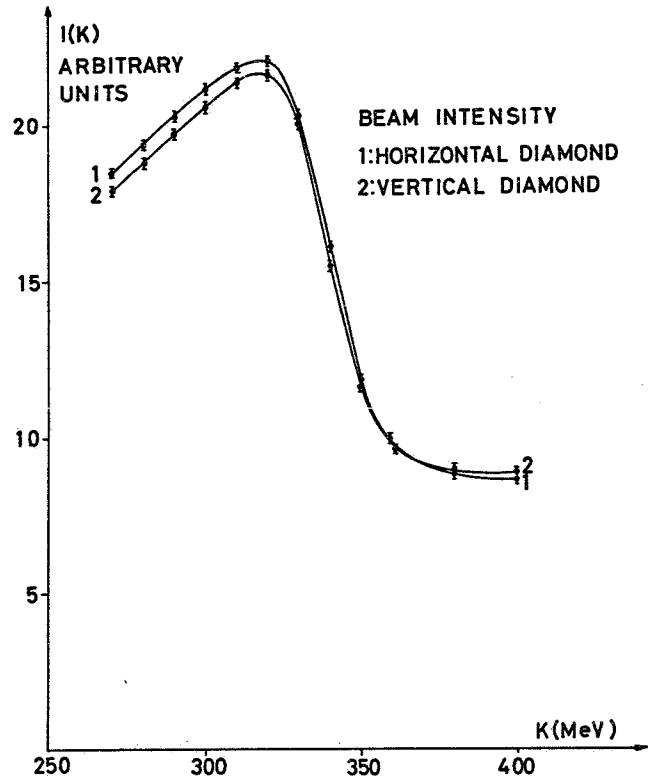

FIG. 1 - Behaviour of the experimental beam intensity I(K) as function of the photon energy K for the two diamonds. I(K) is defined as I(K) = N(K)·K where N(K) is the number of photons per unit energy interval.

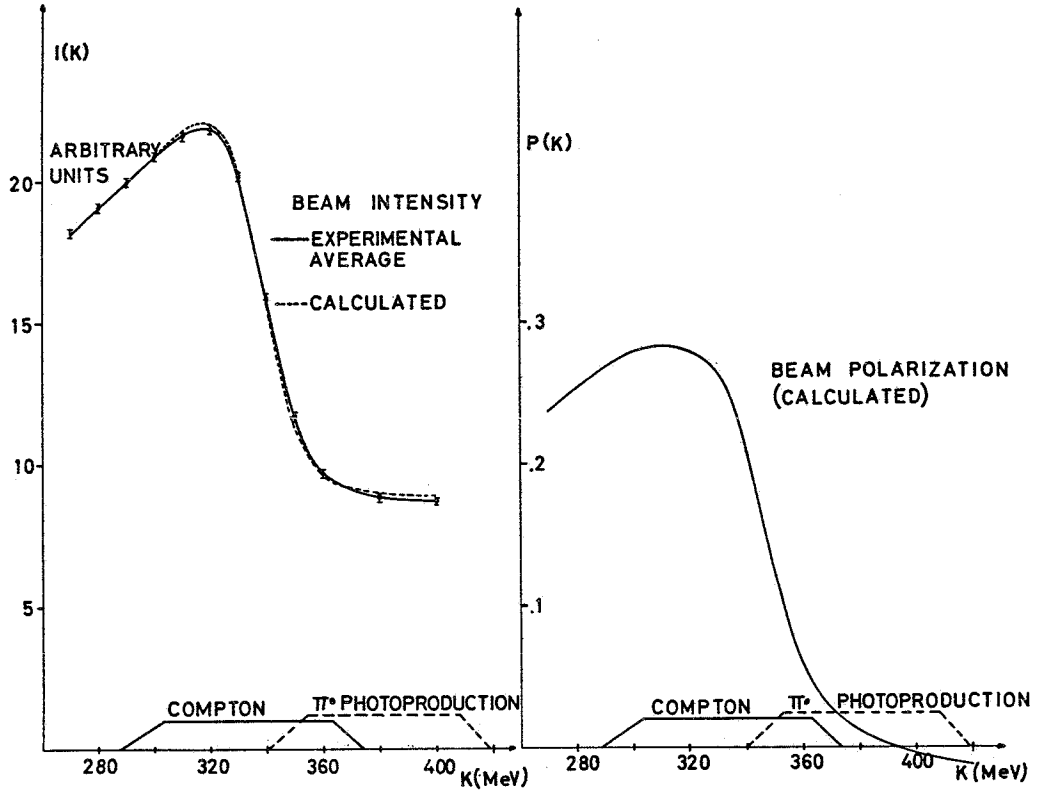

FIG. 2 - Behaviour of the beam intensity, averaged over both diamonds, and of the corresponding polarization P(K) as function of the photon energy K. Along the K axis are shown the intervals which contribute, in our experimental conditions, to Compton effect and π^0 photoproduction. The trapezoidal shape shows efficiency behaviour due to target thickness.

This general procedure for obtaining a reliable value of the polarization has been devised by G. Bologna[2].

The error on the polarization may be due as to the approximations which are present in the calculus as to statistical uncertainties in fitting the experimental spectrum. As a reasonable estimate we have assumed $\Delta P = 0,01$.

Finally we remark that the K interval where the polarization is high enough to allow a measure of $d\sigma_{\parallel}/d\sigma_{\perp}$ with a reasonable error is relatively small: $\sim$ 80 MeV. Therefore it is not possible to obtain an energy behaviour of $d\sigma_{\parallel}/d\sigma_{\perp}$ without changing the setting of the diamond.

EXPERIMENTAL SET UP. -

The observation of the Compton effect is made difficult by the concurrence of π^0 photoproduction.

We separate Compton and π^0 events, following a method previously used by Deutsch et al. [3] comparing the measured photon direction with the one expected according to Compton kinematics. In order to accomplish this, our experimental apparatus has to measure both direction and energy of the proton and the photon direction.

The experimental set up is shown in Fig. 3. The target is a liquid hydrogen cell of 3 x 3 cm^2 cross section and 15 cm length.

At 44° respect to the beam direction we have the proton telescope. It consists of two thin plate spark chambers for direction measurement and of a 20 gaps range spark chamber of total thickness 21 x 0.5 = 10.5 mm of Aluminum. Plastic counters S_1, S_2, S_3 define a stopped proton according to the electronic block diagram of Fig. 4. The S_1 pulse height is analyzed and the S_1 S_2 photomultiplier voltage are adjusted in order to have small pion contamination.

Along the proton path we have two helium bags to decrease proton scattering and therefore the error on its direction.

On the photon direction (75° respect to the beam) we have a veto plastic counter A, a shower spark chamber and an integral lead glass Cerenkov counter C. The shower spark chamber has 2 thin Al plates followed by 19 thick plates (each one being a sandwich of 1 mm Al and 0.5 mm Pb) and finally by other 2 thin Al plates. With it we determine first the conversion point of the photon and after its direction joining this point with the target point obtained extrapolating backwards the proton direction. The conversion efficiency of the shower spark chamber is about 70%.

The master pulse which triggers all the spark chambers

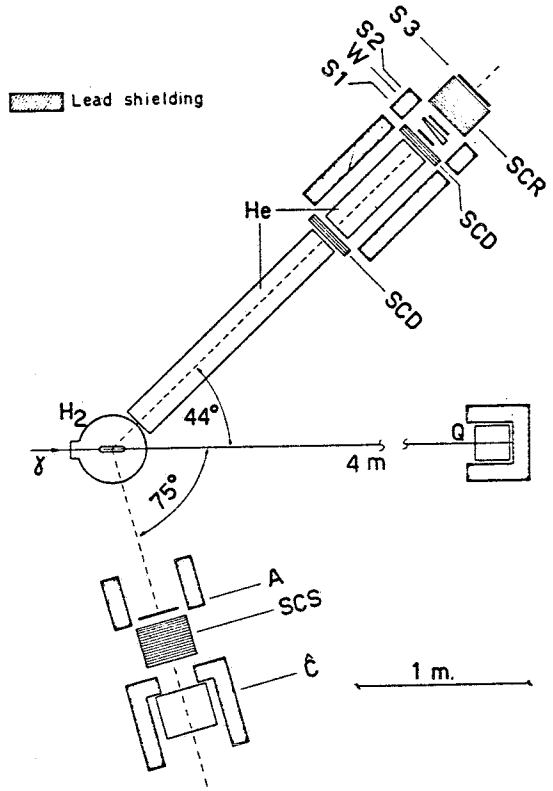

FIG. 3 - Experimental apparatus. Symbols are as follows; SCD: thin plate direction spark chamber ; SCR: range spark chamber; S_1, S_2, S_3: plastic scintillators; W: wedge shaped Aluminum absorber; A: veto plastic scintillator; SCS : shower spark chamber; C: integral lead glass Cerenkov counter; Q: Wilson quantameter.

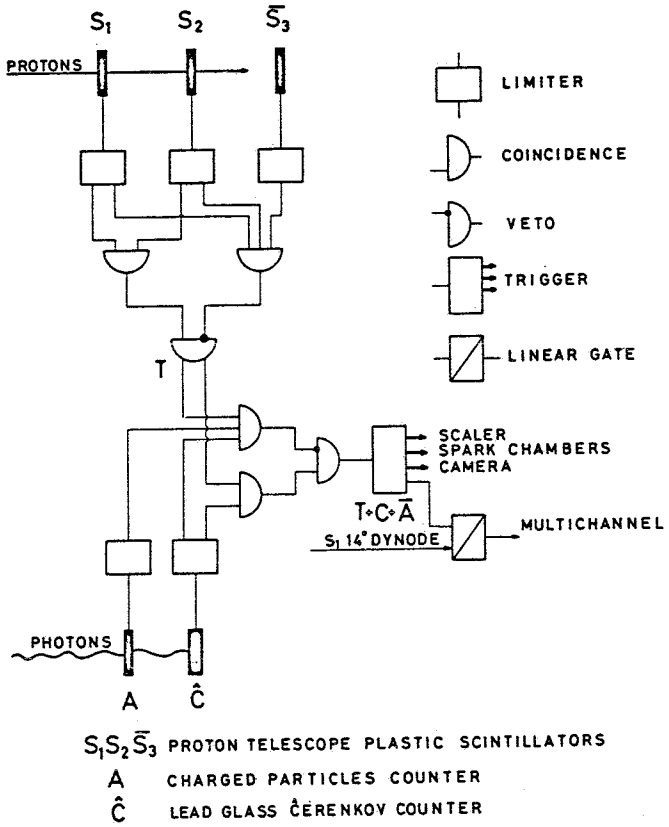

FIG. 4 - Electronic block diagram.

is given by $T + C + \bar{A}$ (see the electronic block diagram on Fig. 4).

The proton solid angle is defined by the S_1 counter and is 0,0021 Sr. The Cerenkov has a solid angle of 0,021 Sr; its geometrical efficiency, averaged over target size, is 84% for Compton events and 7.5% for π^o events. This geometry has been chosen in order to reduce as possible excessive π^o background and get a good Compton ^{o} background separation.

However, as we are measuring a ratio between cross sections, geometrical efficiencies will not affect the final result.

Moreover, in the course of the experiment, we have lost a fraction of the more energetic protons ($\sim$ 20% of the total). In fact the dE/dx values for protons and pions are well separated at counter S_1 (because it is followed by more absorber) while for counter S_2 there is a partial overlap. In order to achieve an efficient pion rejection we have set the S_2 voltage at a relatively low value so that we lose in S_2 a fraction of the protons with lower dE/dx or, that is the same, with higher energy. However this is of no importance for us; first because we are primarily interested to the less energetic protons coming from the polarized region of the γ spectrum and second because we are measuring a ratio between the counting rates.

The energy intervals for the primary photon which contribute to the two reactions are shown in Fig. 2. The spectrum position has been chosen so that the π^o zone falls on the low intensity region and the Compton on the high one. In such a way we may reduce of a factor $\sim$ 2 the ratio π^o background/Compton respect to the use of a conventional bremsstrahlung spectrum.

DATA REDUCTION. -

All our events have been divided in two energy intervals

I interval	$300 \leq K \leq 335$ MeV
II interval	$335 \leq K \leq 370$ MeV

where K is the primary photon energy (calculated according Compton kinematics). It must be emphasized that, there being a 50 MeV energy separation between incoming photons which contribute respectively to Compton effect and to π^o photoproduction (with the same proton kinematics), the π^o events which are classed in these intervals lie respectively in the energy intervals $350 \leq K \leq 385$, $385 \leq K \leq$ $\leq$ 420 MeV.

In the first interval we have the maximum of polarization and for this we will give the ratio of cross sections. Results from the second one will be used as a check because we expect here almost

equal Compton and π^o counting rates owing to the small value of the polarization.

We have collected about 33.000 events of which ~ 21.000 lie in the first interval and ~ 12.000 in the second one.

From the scanning of the pictures of the events we derive the following quantities:

θ_p : proton angle respect to the beam

T_p : proton kinetic energy

$\theta_{\gamma S}$: photon angle respect to the beam.

Then with the formulae of Compton kinematics, we calculate, from θ_p, T_p, the expected photon direction $\theta_{\gamma T}$. Then we define two angular deviations:

$\Delta\theta = \theta_{\gamma T} - \theta_{\gamma S}$

$\Delta\varphi$: angle between planes $(\overline{K}, \overline{p})$ and $(\overline{K}, \overline{K'})$

$\overline{K}$: beam direction

$\overline{p}$: proton direction

$\overline{K'}$: final photon direction.

Notice that, apart from scattering, should be $\Delta\theta = \Delta\varphi = 0$ for Compton events, while for π^o, there being no (two body) correlation between photon measured and expected direction $\Delta\theta$, $\Delta\varphi$, can assume any value compatible with our geometry.

So if we plot the events against $\Delta\theta$, $\Delta\varphi$ the Compton events are contained in a gaussian like peak around $\Delta\theta = \Delta\varphi = 0$ whose width is primarily due to the proton scattering. This peak will be over imposed to the π^o events distribution which is more flat and wide.

In Fig. 7 we present two $\Delta\theta$, $\Delta\varphi$ matrices which show the experimental distribution for the two polarizations. The Compton peak is not centered at 0° because of small errors on the measure of the spark chambers position.

As an aid to the analysis of the experimental distributions of $\Delta\theta$, $\Delta\varphi$ these were also calculated by means of a Monte Carlo method. In the Monte Carlo the experimental conditions are simulated as accurately as possible putting into it the experimental spectrum and the known cross sections for Compton effect and π^o photoproduction(x);

(x) - In Fig. 5 (Fig. 6) are shown the experimental values of interest for Compton[4-7] (π^o photoproduction[8]) unpolarized cross sections and the interpolating curves used for Monte Carlo Calculations. Polarized π^o cross sections were then calculated using the asymmetry measurements reported in ref. (9).

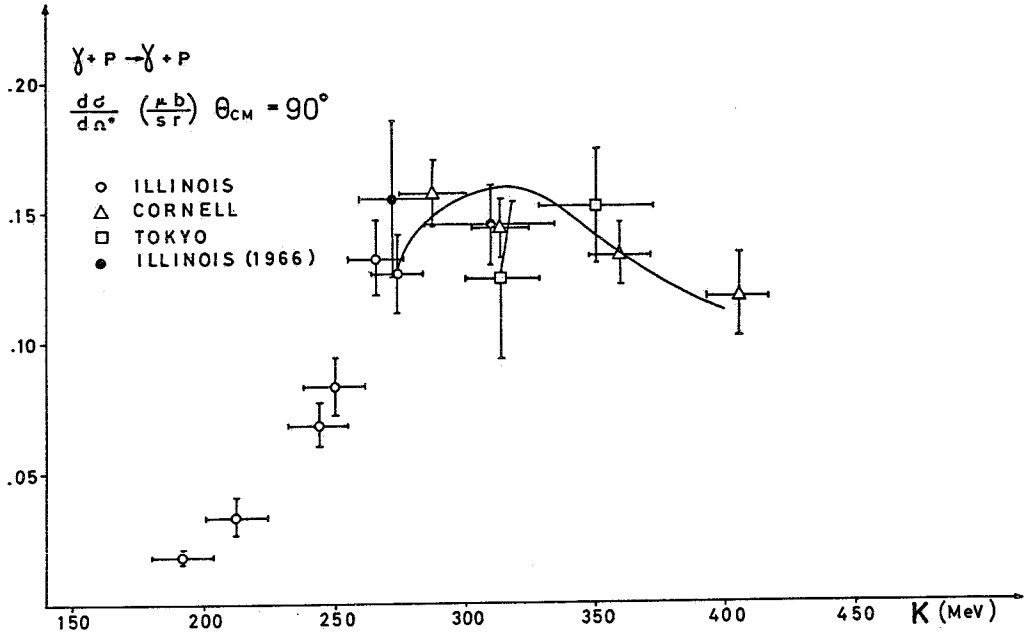

FIG. 5 - Experimental values for 90° C. M. Compton cross sections taken from ref. (4-7). The shown curve has been used for Monte Carlo calculations.

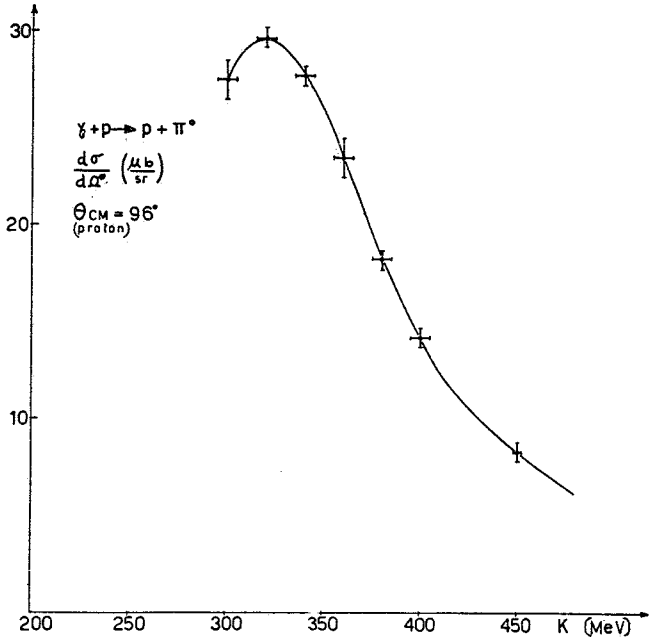

FIG. 6 - Experimental values for θ_p = 96° C.M. π^0 photoproduction cross sections. Data are taken from ref. (8). The shown curve has been used for Monte Carlo calculations.

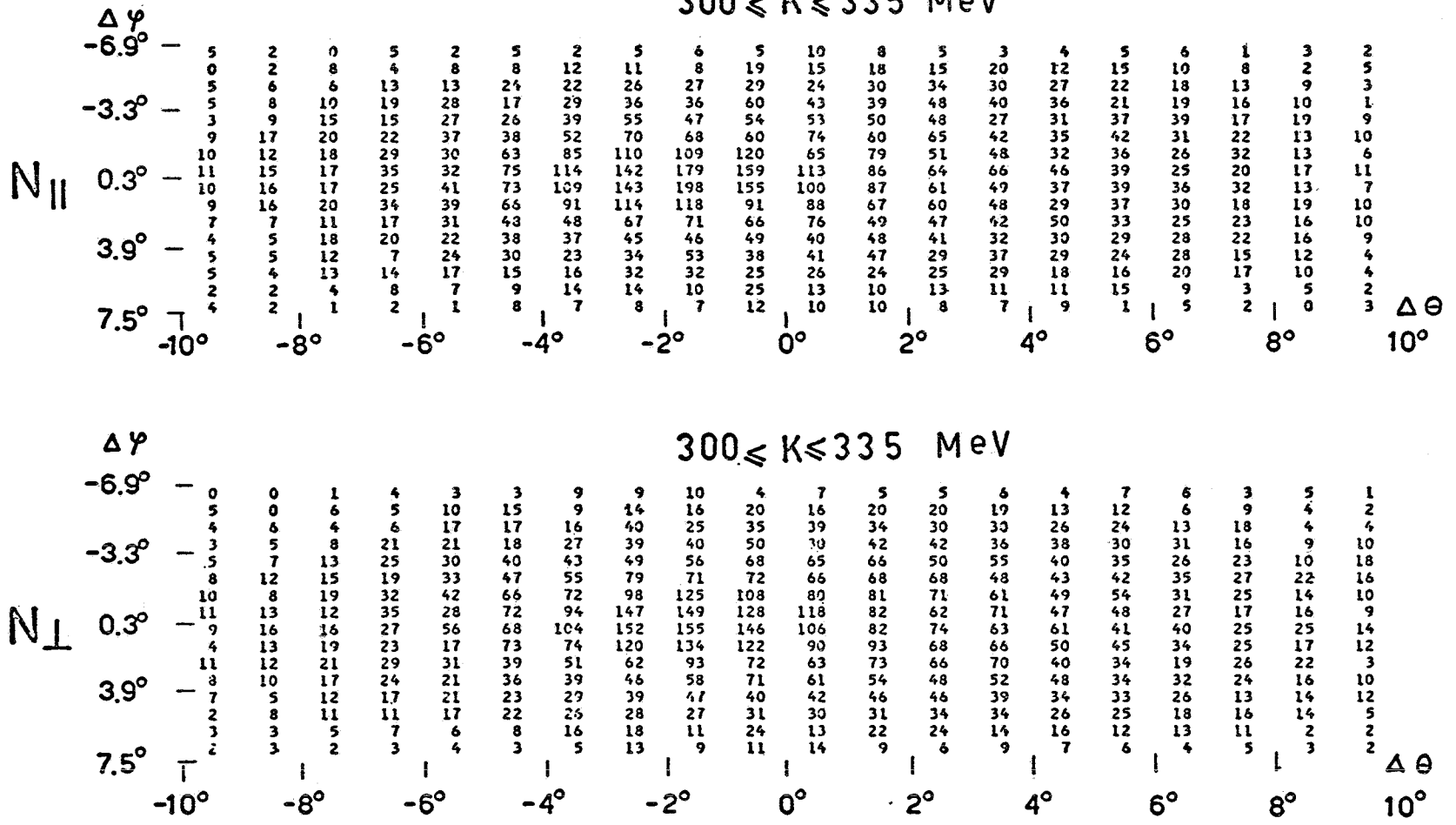

FIG. 7 - Matrix representation of the events distribution versus $\Delta\theta$, $\Delta\varphi$. $N_{\parallel}$, $N_{\perp}$ refer to data collected with the two polarization states. The shown $N_{\parallel}$ matrix is the experimental one multiplied by a factor 0.95 in order to normalize at equal (beam dose x good pictures)/total pictures.

account has been taken of target size, of the proton scattering and, approximately, of edge effects in shower detection.

Becuase of limited computer time the Monte Carlo simulated events are slightly less numerous than the experimental ones. Therefore in the following when necessary the Monte Carlo previsions are accompanied by their statistical error.

We have used the Monte Carlo results in the data analysis in the following way. We assume that the Monte Carlo predicts correctly both for π^o and Compton events, the shape of the $\Delta\theta, \Delta\varphi$ distribution. Then the experimental one shoul be obtained by a linear combination of these two predicted distributions.

Requiring that this combined distribution and the experimental one contain the same number of events we are left with only one free parameter which may be chosen to be the total number of Compton events. Then we have varied this parameter and we have made a χ^2 test confronting the experimental and Monte Carlo distributions.

We find the value of the parameter for which the χ^2 attains the minimum and correspondingly we obtain the separation of the experimental events between π^o and Compton events.

This confront has been carried out in the region $-6,9^o \leq \leq \Delta\varphi \leq +7,5^o$, $7^o \leq \Delta\theta \leq +5^o$ of the matrices of Fig. 7 for each matrix number (except the cases with less than 20 events which were grouped together). The fit is statistically acceptable because the χ^2 values obtained are the following

$N_{\parallel}$: $\chi^2_{min} = 161$ 157 degrees of freedom

$N_{\perp}$: $\chi^2_{min} = 156$ 159 degrees of freedom

The remaining events of the matrix have not been considered because of systematic deviations of the Monte Carlo predictions for the tails of the distribution in $\Delta\theta$. In any case the number of Compton events in this region is surely negligible.

The results of such a procedure are shown in figures 8-9 for a central section of the distribution made along the $\Delta\varphi$ axis.

The separation between Compton and π^o events has been carried out also independently from the Monte Carlo by graphically extrapolating the background shape from the region external to the peak to the region under the peak. This has been done in several ways analysing various sections of the distribution both in $\Delta\theta$ and $\Delta\varphi$. This is shown in Figs. 10-11 where are presented the central sections of the distributions made along $\Delta\theta$. In Figs. 12-13 are reported for confront the sum of the two diamonds distributions: the experimental one and the prediction of the Monte Carlo.

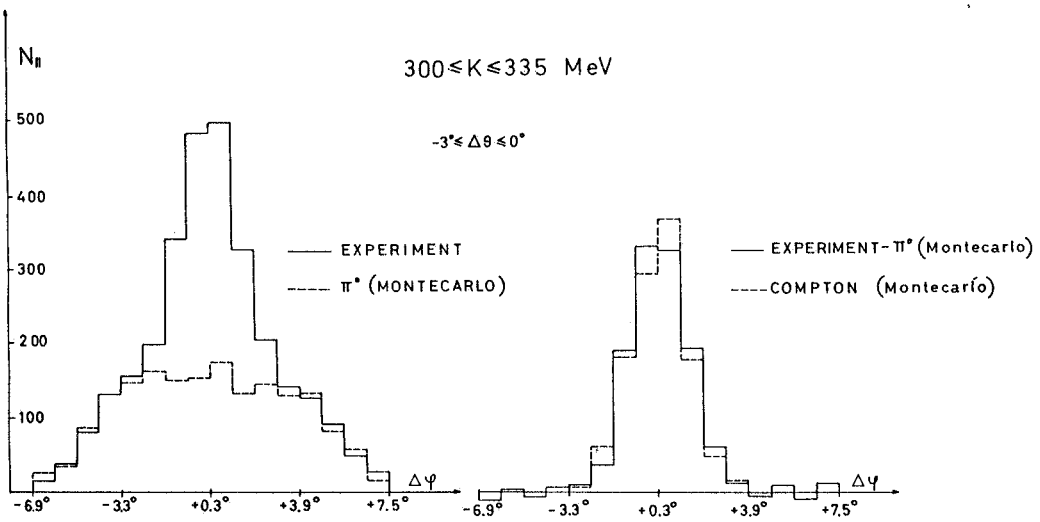

FIG. 8

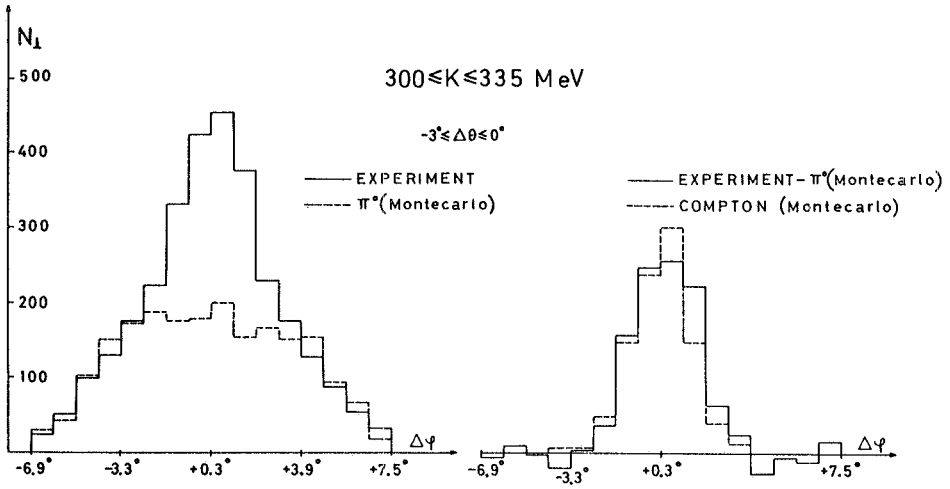

FIG. 8-9 - Distribution versus $\Delta\varphi$ of the events having $-3^{o} \leq \theta \leq 0^{o}$ (this interval is chosen in order to be centered at the maximum of the Compton peak; it contains about 60% of all Compton events). On the left hand side the full line represents the experimental data and the dotted line the π^{o} background estimated using the Monte Carlo - Subtracting this background one obtains for the distribution of the Compton events the full line hystogram shown on the right hand side. There the dotted line represents the Monte Carlo prediction for Compton events.

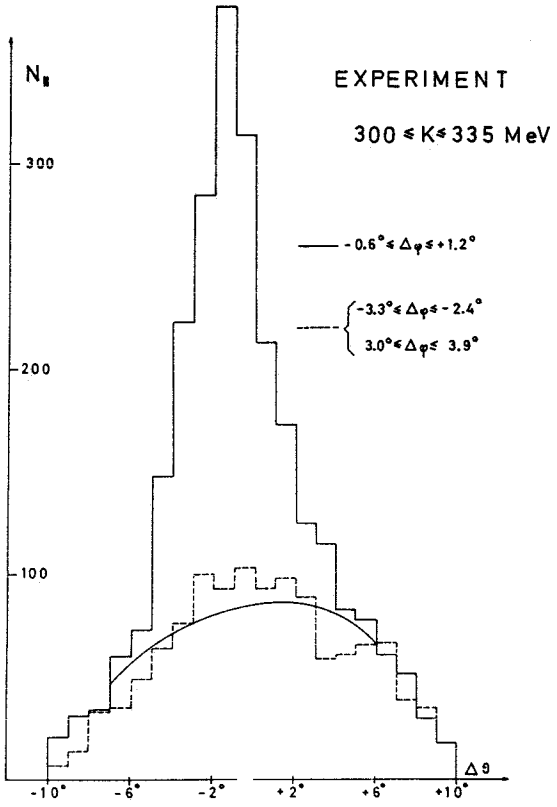

FIG. 10

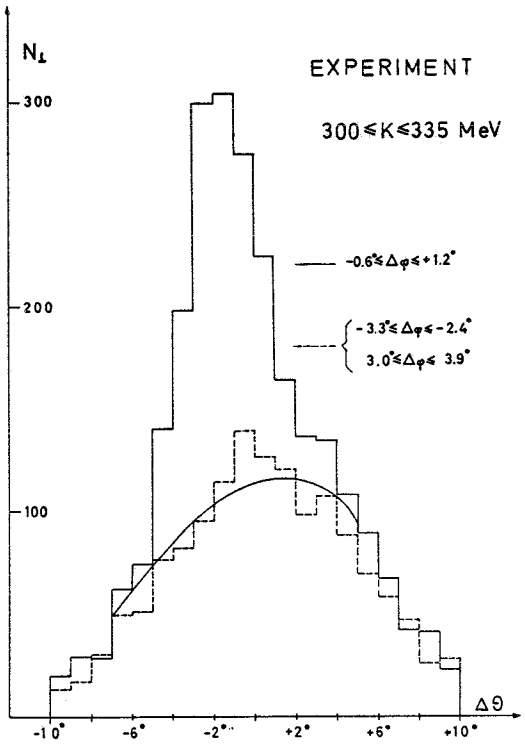

FIG. 11

FIG. 10-11 - Distribution versus $\Delta\theta$ of the events having $-0,6^{o} \leq \Delta\varphi \leq +1,2^{o}$ (full line hystogram) and of the events having $-3,3^{o} \leq \Delta\varphi \leq -2,4^{o}$ and $3,0^{o} \leq \Delta\varphi \leq 3,9^{o}$ (dotted line hystogram). The full line hystogram passes through the Compton peak while the dotted one contains almost only background. We report it to give an idea of the background behaviour. The smooth curve represents the assumed background behaviour. In Fig. 13 are presented the corresponding hystograms predicted by the Monte Carlo together with the predicted π^{o} background under the peak.

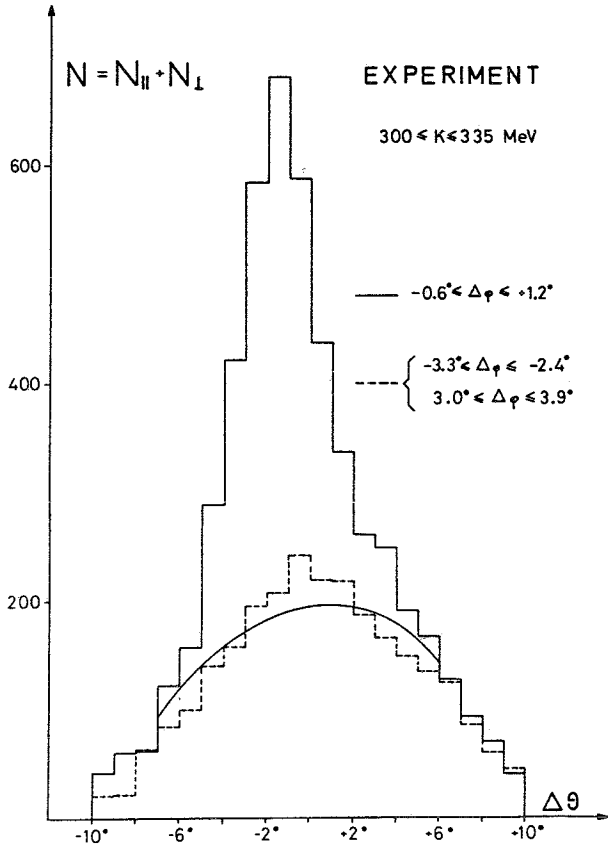

FIG. 12

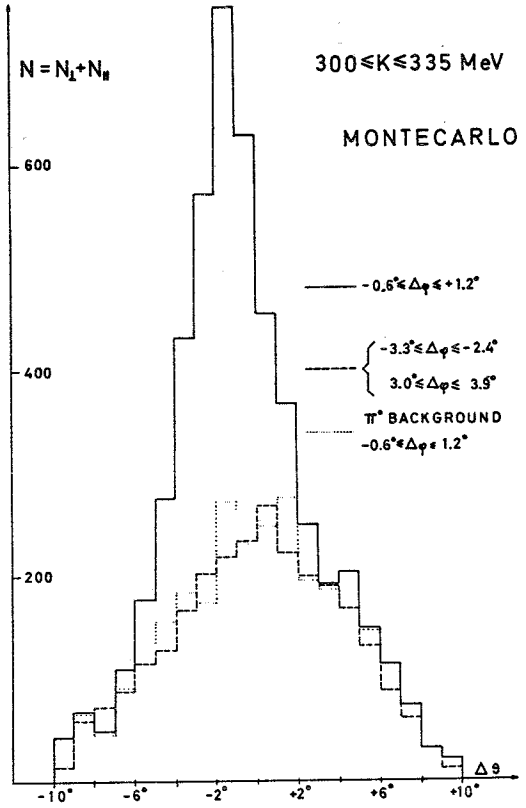

FIG. 13

FIG. 12-13 - Distribution versus $\Delta\theta$ of the events having $-0,6^{o} \leq \Delta\varphi \leq +1,2^{o}$ (full line hystogram) and of the events having $-3,3^{o} \leq \Delta\varphi \leq -2,4^{o}$ and $3,0^{o} \leq \Delta\varphi \leq 3,9^{o}$ (dotted line hystogram). The full line hystogram passes through the Compton peak while the dotted one contains almost only background. We report it to give an idea of the background behaviour. The smooth curve represents the assumed background behaviour. In Fig. 13 are presented the corresponding hystograms predicted by the Monte Carlo together with the predicted π^{o} background under the peak.

The separation of the Compton events from the π^0 events is not free of uncertainties due to the peculiar shape of the $\Delta\theta, \Delta\varphi$ distribution which is the sum of two bell-shaped curves of different width. In effect the use of the Monte Carlo leads to a smaller number of Compton events than the direct background extrapolation. The ambiguity is essentially due to the background level under the Compton peak.

However, both varying the criteria of confront of the data with the Monte Carlo, both following different suggestions for the background extrapolation the ratio $C_{\parallel} / C_{\perp}$ has little dispersion if one takes care to follow the same criteria in making the cut on the data relative to the two diamonds.

A greater $\Delta\theta, \Delta\varphi$ acceptance of our apparatus would probably have made sligthly easier the π^0 Compton separation but would have also required a larger scanning time because of the increased yield of π^0 events.

From the scanning we get also the coordinates of the interaction point in the target. In Figs. 14-15 we show their distribution along the vertical and the longitudinal (parallel to beam) direction together with the curves predicted by the Monte Carlo.

RESULTS. -

We first discuss the results obtained for the polarized region i. e. $300 \leq K \leq 335$ MeV for Compton events to which corresponds the interval $350 \leq K \leq 385$ MeV for π^0 events. For Compton events the value of the polarization averaged over this interval is $P = 0.276$. As said before we assume that the error on the polarization is $\Delta P = 0,01$; however taking account that possible errors in the position of the interval of the accepted energies may lead to errors in the calculation of the average polarization we take a slightly larger error on P and write

$$P = 0.276 \pm 0.014$$

Using the Monte Carlo results as described before we find:

$$C_{\parallel} = 1975 \pm 70 \qquad \pi^0_{\parallel} = 8170 \pm 100$$
$$C_{\perp} = 1620 \pm 60 \qquad \pi^0_{\perp} = 9255 \pm 95$$

The errors are statistical in nature and include both the counting statistical error both the statistical uncertainty in setting the level of the π^0 background. They are computed following the formulas given by Moravcsik and Cziffra[10] for the errors on the coefficients when using

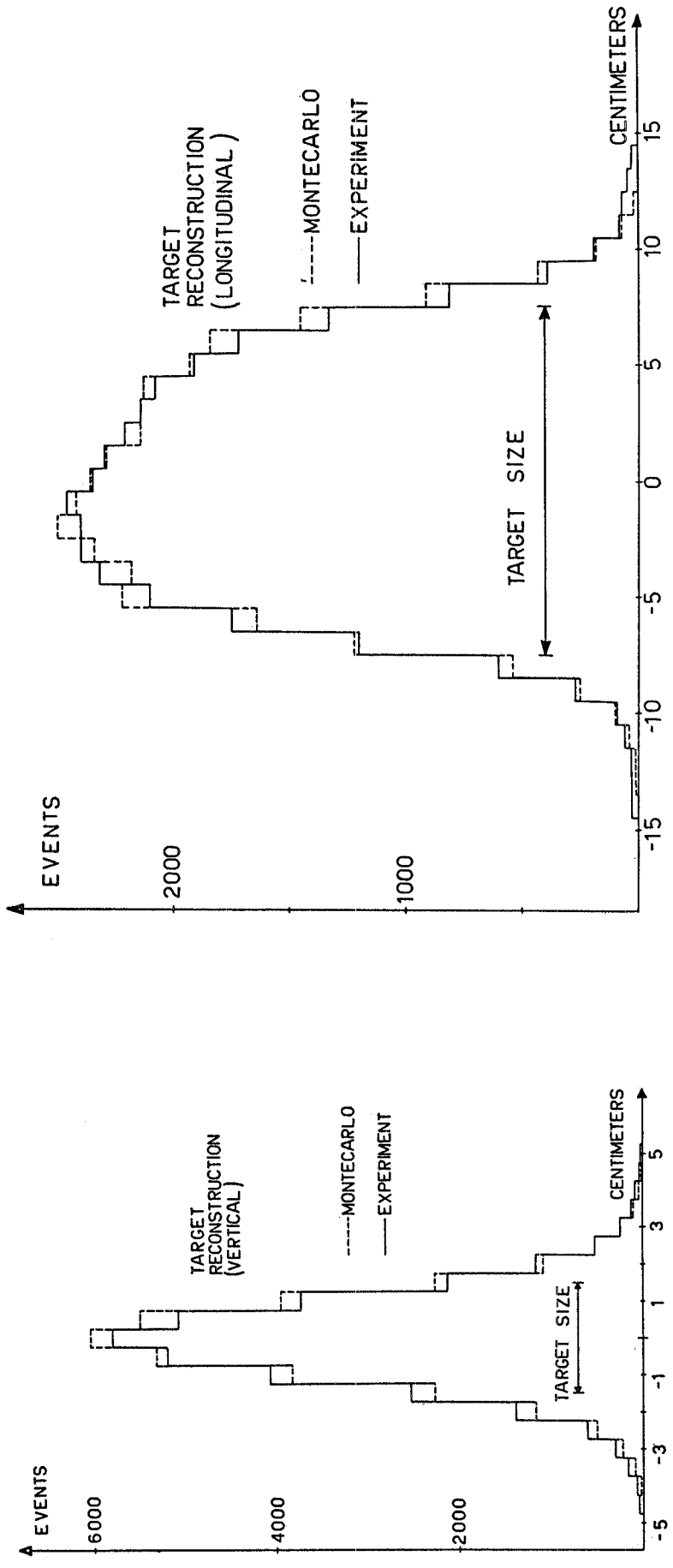

FIG. 14

FIG. 15

FIG. 14-15 - Distribution in the median vertical plane of the target of the interaction points, as reconstructed from the pictures scanning. Fig. 19 refers to the vertical distribution and Fig. 20 to the one along beam axis.
Dotted lines represent the Monte Carlo previsions.

the least squares method.

All these numbers refer to the same dose.

For the ratio we then obtain:

$$R_C = \frac{C_{\parallel}}{C_{\perp}} = 1,22 \pm 0,06$$

Using the direct extrapolation of the background we get for C and C higher numbers:

$$C_{\parallel} \simeq 2450 \qquad C_{\perp} \simeq 2030$$

and a ratio $C_{\parallel}/C_{\perp} = 1,21$ which is in agreement with the previous one. We stress here again the fact that the uncertainty on the exact background shape may lead to rather large errors on the absolute yields of $C_{\parallel}$ and $C_{\perp}$; however if one takes care to use the same criteria for both the $\parallel$ and $\perp$ distributions the influence of the sistematic error due to background overestimation or underestimation is small on the ratio R_C.

Inserting the value of R_C in formula (1) together with the value of the averaged polarization we get:

$$R_{\sigma} = 2,1 \begin{matrix} +.5 \\ -.4 \end{matrix}$$

where the errors are computed quadratically combining the errors due to R_C and P (this last one is however less important).

CONSISTENCY CHECKS. -

Summing the results of both diamonds we get the overall background to Compton ratio:

$$\frac{\pi^0}{C} = \frac{\pi^0_{\parallel} + \pi^0_{\perp}}{C_{\parallel} + C_{\perp}} = 4.85 \pm 0.15$$

The quoted error is only the statistical one. Here systematic errors in background separation are very important. The Monte Carlo prediction for it is $5,2 \pm 0,15$ and has been calculated using the values for the cross sections shown in Figs. 5, 6. The partial disagreement could also be due to inappropriate choice of the curve fitting the measured Compton cross sections whose behaviour at the resonance is not well known since the experimental data have large errors.

Also the $\pi^0_{\parallel}$, $\pi^0_{\perp}$ counts show an asymmetry due to the

presence of a net polarization also in the region $350 \leq E_\gamma \leq 385$ MeV. We recall that for π^0 photoproduction the asymmetry is in the opposite direction respect to the Compton effect and its value is $d\sigma_\perp / d\sigma_\parallel \simeq -4$ at the resonance. Inserting in the Monte Carlo the known π^0 asymmetry[9] we obtain: $\pi^0_\perp / \pi^0_\parallel = 1.12 \pm 0.05$ which is in excellent agreement with the experimental result:

$$\frac{\pi^0_\perp}{\pi^0} = 1,13 \pm 0,02.$$

For the low polarization region ($335 \leq K \leq 370$ MeV for Compton, $385 \leq K \leq 420$ MeV for π^0 events) the data analysis was carried on in the same way and here we quote the results obtained using the Monte Carlo:

$$C_\parallel = 800 \pm 50 \qquad \pi^0_\parallel = 5160 \pm 75$$
$$C_\perp = 750 \pm 45 \qquad \pi^0_\perp = 5390 \pm 70$$

The experimental ratios are therefore the following:

$$\frac{C_\parallel}{C_\perp} = 1.07 \pm 0.09 \qquad \frac{\pi^0_\perp}{\pi^0_\parallel} = 1.045 \pm 0.020$$

While the Monte Carlo predictions are

$$\frac{\pi^0_\perp}{\pi^0_\parallel} = 1.05 \pm 0.05$$

The ratio $C_\parallel / C_\perp$ is near to 1 as expected from the low value of the polarization.

COMPARISON WITH THEORY. -

We show in Fig. 16 our experimental value of $d\sigma_\parallel / d\sigma_\perp$ together with some theoretical curves. Curves (a), (b), (c) refer to calculations based on an isobaric model used by Nagashima[11], considering contributions from various intermediate states. Curve (d) is the prevision of the dispersive theory[12, 13], whose range of validity, however, ends at near 270 MeV. We reproduce it to show that the more refined calculations based on dispersion theory give results not in disagreement with the simple isobaric model. Curve (e) is derived from Berkelman, phenomenological model[14].

Assuming [15] that the only multipole contributing to the transition is the magnetic dipole M_{1+} one gets $d\sigma_\parallel / d\sigma_\perp = 2,5$.

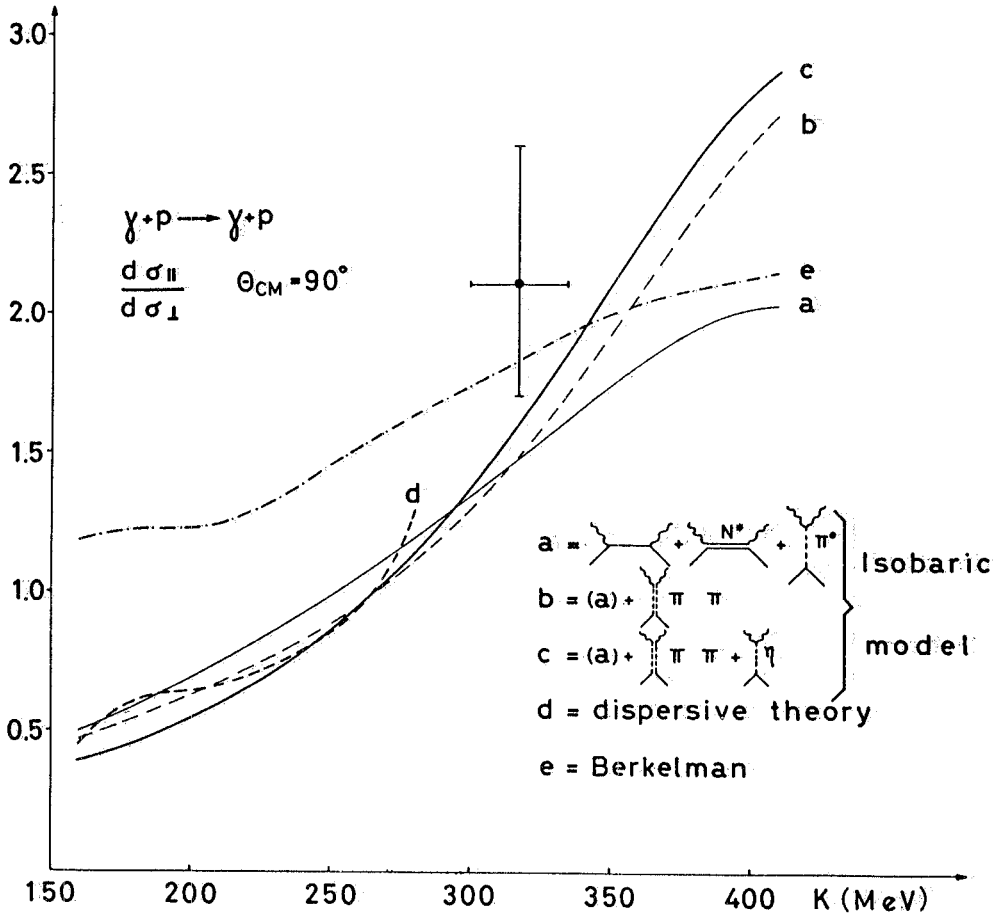

FIG. 16 - Our experimental result is compared to various theoretical curves. Curves a), b), c) have been calculated by us with the isobaric model following ref. (9). Curve d) is takes from ref. (11) and curve e) from the Berkelman work (12).

ACKNOWLEDGEMENTS. -

We like to mention here that for the preliminary part of the work Prof. G. Diambrini and Prof. G. Bologna were kindly collaborating with us.

We thank Prof. G. Bologna also for giving us the program for spectrum calculation and Dr. F. Fabbri for help in the calculations.

Thanks are due to the Synchrotron staff for assistence during the machine runs and to the Istituto Superiore di Sanità for computer time.

Finally we are indebted to Mr. G. Di Stefano and coworkers for their excellent technical work.

REFERENCES. -

(1) - G. Barbiellini, G. Bologna, G. Diambrini and G. P. Murtas, Phys. Rev. Letters 8, 112 (1962).
(2) - G. Bologna (to be published)
(3) - R. F. Stiening, E. Loh and M. Deutsch, Phys. Letters 10, 536 (1963).
(4) - C. Bernardini et al., Nuovo Cimento 18, 1203 (1960).
(5) - J. W. De Wire et al., Phys. Rev. 124, 909 (1961).
(6) - Y. Nagashima, Ph. D. Thesis, Tokyo (1964).
(7) - E. R. Gray, Ph. D. Thesis, Urbana, Illinois (1966).
(8) - J. T. Beale et al., report CTSL-42, Caltech (1966).
(9) - A. Donnachie and G. Shaw, Ann. Phys. 37, 333 (1966).
(10) - P. Cziffra and M. J. Moravcsik, UCRL-8523.
(11) - Y. Nagashima, Progr. Theor. Phys. 33, 828 (1965).
(12) - M. Jacob and J. Mathews, Phys. Rev. 117, 854 (1960).
(13) - A. Santroni, report 66/2 A. E. B. - 11, Genova University (1966).
(14) - K. Berkelman, Nuovo Cimento 21, 633 (1961).
(15) - A. Verganelakis, Nuovo Cimento 31, 1121 (1964).